(4) Paine, A. J. *J. Polym. Sci., Part A: Polym. Chem.*, accepted.
(5) Paine, A. J.; McNulty, J. *J. Polym. Sci., Part A: Polym. Chem.*, accepted.
(6) Barrett, K. E. J., Ed. *Dispersion Polymerization in Organic Media*; Wiley-Interscience: New York, 1975.
(7) Corner, T. *Colloids Surf.* **1981**, *3*, 119.
(8) Ober, C. K.; Lok, K. P. *Macromolecules* **1987**, *20*, 268.
(9) Ober, C. K.; van Grunsven, F.; McGrath, M.; Hair, M. L. *Colloids Surf.* **1986**, *21*, 347.
(10) Lok, K. P.; Ober, C. K. *Can. J. Chem.* **1985**, *63*, 209.
(11) Almog, Y.; Reich, S.; Levy, M. *Br. Polym. J.* **1982**, *14*, 131.
(12) Tseng, C. M.; Lu, Y. Y.; El-Aasser, M. S.; Vanderhoff, J. W. *J. Polym. Sci., Part A: Polym. Chem.* **1986**, *24*, 2995.
(13) Susoliak, O.; Barton, J. *Chem. Pap.* **1985**, *39*, 379.
(14) Lu, Y. Y.; El-Aasser, M. S.; Vanderhoff, J. W. *J. Polym. Sci., Part B: Polym. Phys.* **1988**, *26*, 1187.
(15) Paine, A. J. *Macromolecules*, accompanying paper in this issue.
(16) Reference Manual for the Coulter Multisizer, Issue A: October 1986. Part No. 9903623 from Coulter Electronics Ltd., Luton, U.K.
(17) Paine, A. J. Presentation at Lehigh University, Oct 5, 1987.
(18) Flory, P. J. *Principles of Polymer Chemistry*; Cornell University Press: Ithaca, NY, 1953.
(19) Smoluchowski, M. V. *Z. Phys. Chem.* **1917**, *192*, 29.
(20) Piirma, I., Ed. *Emulsion Polymerization*; Academic Press: New York, 1982.

Registry No. PVP, 9003-39-8; polystyrene, 9003-53-6.

Dispersion Polymerization of Styrene in Polar Solvents. 7. A Simple Mechanistic Model To Predict Particle Size

Anthony James Paine

Xerox Research Centre of Canada, 2660 Speakman Drive, Mississauga, Ontario, Canada L5K 2L1

Received September 27, 1989

ABSTRACT: An integrated model for dispersion polymerization is developed to predict particle size from first principles. The key components of this model are a multibin kinetic model for unstabilized particle coalescence, the grafting mechanism of stabilization, and the radius of gyration of the grafted stabilizer chains. A critical point is defined where similar-sized particles stop coalescing with one another because the graft available equals the minimum graft required to stabilize the particles. Examples indicate that the particle count is determined within the first 1% of conversion, in agreement with experiment, and that the critical size particles are larger than 0.1 μm—significantly bigger than nuclei. In cases where full adsorption of graft is likely, absolute prediction of particle size is remarkably consistent with experiment. More generally, however, partial adsorption of graft is likely to affect the predicted scaling of diameter with stabilizer, initiator and monomer concentrations, and stabilizer molecular weight. Above the critical size, the size distribution narrows because the growing particles continue to capture dead polymer formed in solution. Observed loss of monodispersity by stabilization of secondary particles or coalescence of large particles is readily explained with this model. A critical factor influencing the final size distribution is the locus of polymerization and how it changes during the reaction.

During dispersion polymerizations latex particles are formed from an initially homogeneous reaction mixture by polymerization in the presence of a suitable steric stabilizer polymer.[1-17] In hydrocarbon solvents, poly(dimethylsiloxane), poly(isobutylene), poly(12-hydroxystearic acid), and poly(2-ethylhexyl methacrylate) have been employed as stabilizers for polymerization of methyl methacrylate.[7-11] Styrene monomer has been polymerized in alcohols with steric stabilizers such as (hydroxypropyl)cellulose (HPC), poly(acrylic acid) (PAA), or poly(*N*-vinylpyrrolidone) (PVP).[1,4,6,12-17] In favorable circumstances, these particles can have a very narrow, or even monodisperse, size distribution.

Our previous work on the dispersion polymerization of styrene in alcohols had focused primarily on HPC and, more recently, on PVP as steric stabilizer.[1-6] These efforts continued work initiated by Ober, Lok, and Hair (HPC and PAA),[13-15] Almog et al. (PVP and others),[17] and Vanderhoff and El-Aasser et al. (PVP).[16] Although a costabilizer (anionic or nonionic surfactant) was employed with PVP in the investigations by Vanderhoff and El-Aasser, recent evidence suggests that this additive has no influence on the outcome of the reaction in most of the parameter space investigated.[5] The gross features of the HPC- and PVP-stabilized reactions are substantially similar and are comparable to reactions stabilized by PAA, poly(vinyl butyral), and poly(*N*-vinylpyridine).[18]

The preceding work by us and others has shown the mechanism of dispersion polymerization to be complex and poorly understood. It is known that the particle count is fixed very early in the reaction, before 2–5% conversion, and that, at this point, the particles are already monodisperse. Stabilizer, stabilizer concentration, monomer concentration, initiator, and solvent all play important roles in determining the ultimate particle size and molecular weight of the product. To date, mechanistic models of the process are qualitative in nature. Some are sensible on an intuitive basis, but none are quantitatively useful for predicting the particle size and size distribution—properties of the greatest interest.

Three key aspects of any mechanistic model are (1) the mechanism of stabilization, (2) the role of solvent, and (3) the locus of polymerization.

1. For polymerization of styrene in polar solvents stabilized by HPC, we found that the steric stabilizer becomes grafted and ends up on the particle surface.[1-3] Dispersion-polymerized particles may be dissolved in a good solvent such as dioxane and precipitated with a solvent that is poor for polystyrene but good for the steric stabilizer to generate new particles with similar surface-bound HPC.[1-3]

2. The effects of solvent seem to be related to the solubility properties of the grafted stabilizer—the greater its solubility, the larger the particle size.[4] Indeed, the

0024-9297/90/2223-3109$02.50/0

trend of increased particle size with increasing monomer concentration appears to be primarily a solvent effect.[6]

3. Locus of polymerization studies by Ober and Hair[19] and by Vanderhoff and El-Aasser[20] described the distribution of monomer between solution and particle phases during the reaction and concluded that polymerization occurs in both. Frequently observed inverse correlations between particle size and molecular weight can be accounted for by changes in the locus of polymerization: the greater number density of smaller particles ensures that they efficiently capture growing oligomeric radicals initiated in solution, leading to solid-phase polymerization of high molecular weight because of the gel effect. On the other hand, larger particles capture dead polymer that terminated in the continuous phase, with a molecular weight typical of solution polymerization.[6] This is more complex than emulsion polymerization, where the locus of initiation is in the aqueous phase, reasonable steady-state assumptions can be maintained throughout the reaction, and polymerization occurs in the particle phase.[21]

While understanding these three key aspects in a qualitative way helps to rationalize observed trends, there is still a need for an integrated model capable of predicting the final particle size and size distribution. Why are monodisperse particles formed? Why are polydisperse particles sometimes formed? What is responsible for the observed scaling of particle size with initiator concentration, stabilizer concentration, and stabilizer molecular weight?

The objective of this paper is to develop a semiquantitative model capable of addressing these questions. Our evolutionary approach will be (1) to examine unstabilized reactions, (2) to predict particle size from stabilized reactions generating monodisperse particles, (3) to compare the model with experimental results, and then (4) to account for loss of monodispersity.

1. Unstabilized Solution Polymerization and Precipitation

In the absence of steric stabilizer, polymerization of styrene in alcohols gives coagulum with molecular weight very close to that expected for solution polymerization. The absence of any gel effect on the molecular weight under these conditions suggests that the oligomeric radicals terminated in solution prior to capture by the coagulum. Whether these dead polymer chains were captured as nucleated globules or as random or collapsing coils is not important. What is important is that most of the polymer was dead when captured.

In the early part of the reaction, the volume fraction of polymer is low, and the distribution coefficients of monomer and initiator are not strongly biased toward either the continuous or particle phase.[19,20] As a result, the vast majority of early polymerization occurs in solution. To the extent it is possible to ignore oligomeric radical capture by growing particles in the very early part of the reaction, growth by aggregation and coalescence can be decoupled from polymerization, for separate study, as discussed below.

Multibin Particle Aggregation Model. Related work by Hansen and Ugelstad[22] and Napper and Gilbert[23] on emulsion polymerization, Suzuki et al. on the coagulation of oil droplets,[24] and Marqusee on Ostwald ripening[25] led us to develop the following highly simplified model for particle aggregation or coalescence. In the limit of low conversion, where solution polymerization is dominant, dead polymer chains of chain length CL are generated by a pseudo-zero-order rate, k_1, and then coalesce irreversibly at a diffusion-controlled rate. By simulating the kinetics of this model process, we gain insight into a variety of features of dispersion polymerization.

One of the difficulties inherent in modeling particle aggregation is the need to keep track of various populations for particles from newly formed nuclei up to particles of 10 μm or more (i.e., aggregation of species from 1 to 10^{10} chains). Even with modern computing capacity, there are too many species to track individually, so a method is required to group them. The best grouping method is a geometrical progression of population bins such that, for example, the particles in bin $j + 1$ are double the mass of those in bin j. In this case, bin 1 is assigned to the single-chain nuclei and 20–30 bins cover the whole size range.

With this concept, it is a simple matter to generate the rules governing particle coalescence: two particles of the same size (i.e., both in bin j) coalesce to form one particle in the next higher bin $(j + 1)$; particle coalescence of one large and one small particle (i.e., one from bin j and one from bin i, where $i < j$) do not significantly alter the size of the particle in bin j but do bring more mass into the bin and decrease the mass and number count in bin i. These rules can be expressed more explicitly by the following differential equations for the number, n_j, the total mass, m_j (in units of number of polymer chains), and the total square of the masses, $\langle m_j^2 \rangle$, of particles in any bin:

$$dn_j/dt = {}^1/_2 k_{j-1,j-1} n_{j-1}^2 - k_{j,j} n_j^2 - n_j \sum_{i>j} k_{ij} n_i + 0 \quad (1)$$

$$dm_j/dt = k_{j-1,j-1} m_{j-1} - k_{j,j} m_j n_j - m_j \sum_{i>j} k_{ij} n_i + n_j \sum_{i<j} k_{ij} m_i \quad (2)$$

$$d\langle m_j^2 \rangle/dt = k_{j-1,j-1}(m_{j-1}^2 + n_{j-1}\langle m_{j-1}^2 \rangle) - k_{j,j}\langle m_j^2 \rangle n_j - \langle m_j^2 \rangle \sum_{i>j} k_{i,j} n_i + \sum_{i<j} k_{i,j}(n_j \langle m_i^2 \rangle + 2 m_i m_j) \quad (3)$$

For the first bin, containing the "nuclei", the formation terms are replaced by a pseudo-zero-order rate of generation of single dead chains, k_1, which can be related to conventional solution kinetics by, for example, $k_1 = fk_d[I]$:

$$\frac{dn_1}{dt} = \frac{dm_1}{dt} = \frac{d\langle m_1^2 \rangle}{dt} = k_1 - k_{11} n_1^2 - n_1 \sum_{i>1} k_{i,1} n_i + 0 \quad (4)$$

The four terms in eqs 1–4 correspond to (a) coalescence of particles in the preceding bin, (b) coalescence of particles in bin j, (c) capture of particles in bin j by larger particles, and (d) capture of smaller particles, respectively. The three derivatives in eq 4 are numerically (though not dimensionally) equal; by definition $\langle m_1^2 \rangle = m_1 = n_1$. The size-dependent rate constants, k_{ij}, incorporate diffusional factors and stability information. From these equations, one can calculate the number-average mass of a particle in bin j as m_j/n_j and the weight-average mass as $\langle m_j^2 \rangle / m_j$. The overall number-average particle mass, N, and weight-average mass, M, can be related to the size, d, given chain length, monomer molecular weight, and geometrical factors by eqs 5a–c.

$$N = \sum_i m_i / \sum_i n_i \quad (5a)$$

$$M = \sum_i \langle m_i^2 \rangle / \sum_i m_i \quad (5b)$$

$$d = \left(\frac{6N(\mathrm{CL})\mathrm{MW_s}}{\pi \rho N_A} \right)^{1/3} \quad (5c)$$

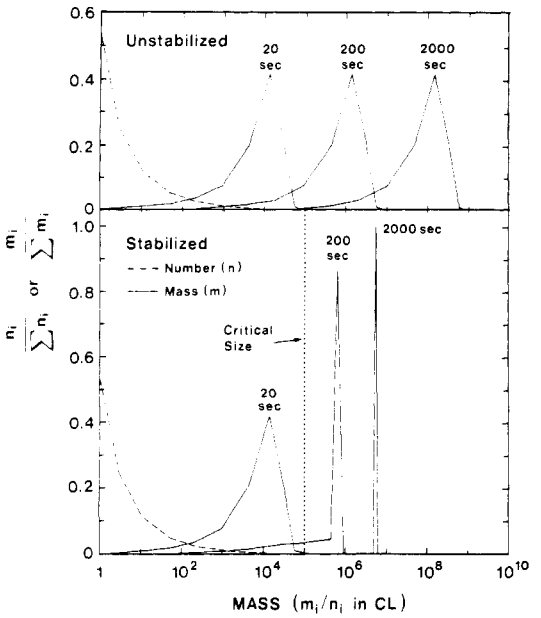

Figure 1. Time evolution of typical number and volume distributions for unstabilized (top) and stabilized (bottom) simulations with $k_1 = 10^{-7}$ and $k_2 = 10^9$. The latter simulation assumed that particle coalescence terminated when two colliding particles were both larger than a critical size of 10^5 chains of length CL. The number distributions are not distinguishably different from each other on this scale and lie on the same dashed curve. Note the geometric self-similarity of the volume distributions in the top set and the narrowing of the size distribution above the critical size in the bottom set.

In our simulations, we computed the cumulative volume distribution to find the median diameter, d_{50}, and the geometric standard deviation (GSD = $(d_{84}/d_{16})^{1/2}$), which can be compared to experimental Coulter counter measurements.

This simple picture describes uncontrolled coalescence of dead polymer particles in unstabilized reactions. To investigate the properties of the numerical system, we made several simplifying assumptions: (a) dead polymer was generated in bin 1 from solution with pseudo-zero-order rate constant k_1 (reasonable values are 10^{-6}–10^{-8} mol L^{-1} s^{-1}, corresponding to the rate of initiation); and (b) aggregation was Smoluchowski diffusion controlled,[26,27] with rate constant k_{ij} proportional to the product of the sum of the diffusion constants, D_i and D_j, times the sum of the particle diameters, d_i and d_j. For hard spheres, D_i is also proportional to d_i^{-1}, so k_{ij} depends only on the diameters of the coalescing particles: $k_{ij} = k_2(1/d_i + 1/d_j)(d_i + d_j)/4$. Reasonable values for k_2 or k_{ii} are 10^8–10^{10} mol L^{-1} s^{-1} (for diffusion-controlled processes). Runge Kutta integration[28] of the number and mass differential equations describing the various bins leads to the following results, as shown in Figure 1, top:

1. Around 20–30 bins (60–90 differential equations) are required to describe the particles, and the average particle mass in each bin increases by a factor of slightly more than 2 per bin.

2. The particle population can be visualized in two classes: very small aggregates of 1–10 chains (bins 1–4, which account for most of the number distribution), and a group of much larger growing particles containing many thousands of chains (which account for most of the mass or volume distribution—see Figure 1, top). These larger particles form the macroscopically observable system, and they capture smaller particles and aggregates before they can form intermediate-sized particles. Thus, after an initial short burst of particle formation, no new growing particles are created and those already in existence are growing by coalescing with each other and by scooping up the steady-state supply of new nuclei.

3. The GSD of the growing particles evolves quickly and remains constant at around 1.5. This leads to the geometric self-similarity in the upper portion of Figure 1 from which simple equations relating particle size to k_1, k_2, and time can be derived. The mean particle mass of the growing particles increases with the second power of time, so the diameter of the particles grows with the 2/3 power of time, and the number of growing particles *decreases* with the first power of time, as shown in eqs 6–10 (where the meaning of the symbols is explained in the appendix). For comparison, the theory of Ostwald ripening shows radius growing as $t^{1/3}$ and N_p decaying as t^{-1} (ref 25). This is in good agreement with these results when the steady generation of new material is factored out. The value of the simulation is simply to provide the constant of proportionality 0.386, in eq 6.

$$d_{50}^3 = 0.386\frac{6MW_s(CL)}{\pi\rho N_A}k_1k_2t^2 \tag{6}$$

We may convert from time base, t, to conversion base, x, with eq 7; use the definition $k_1 = fk_d[I]$ and the relation for chain length, $CL = k_p[M](k_tfk_d[I])^{-1/2}$ (assuming negligible chain transfer), to transform eq 6 into eq 8:

$$x = k_pt\left(\frac{fk_d[I]}{k_t}\right)^{1/2} \tag{7}$$

$$d_{50}^3 = 0.386\frac{6MW_s[M]k_2}{\pi\rho k_pN_A}\left(\frac{k_t}{fk_d[I]}\right)^{1/2}x^2 \tag{8}$$

The number of particles at any conversion is N_p, given by eqs 9 and 10, by substitution from eq 8.

$$N_p\frac{d_{50}^3\pi}{6} = \frac{x[M]MW_s}{\rho} \tag{9}$$

$$N_p = \frac{N_Ak_p}{0.386k_2x}\left(\frac{fk_d[I]}{k_t}\right)^{1/2} \tag{10}$$

These relationships are durable over wide ranges of values for k_1 and k_2. The ultimate product of unstabilized coalescence is a single particle—equivalent to coagulum, as observed.

2. A Model for Stabilized Reactions Giving Monodisperse Particles

Multibin Kinetic Model. The foregoing discussion provided the background against which we can begin to evaluate the effect of stabilizer on dispersion polymerization. The simplest extension of the preceding model is one where same size particle coalescence (homocoagulation) is numerically terminated at some arbitrary critical size, d_{crit}. At this point, the formerly unstabilized reaction becomes stabilized, and only small-particle capture (heterocoagulation) can continue. In this case, simulations show that a monodisperse size distribution evolves after the critical point, because the diffusion-controlled scavenging of dead polymer allows smaller particles to grow faster, catching up to the larger particles. This is illustrated in Figure 1, bottom.

Once the particles become monodisperse, the simulation shows the particle count is constant, and particle diameter grows with time to the 1/3 power, as expected. It takes about 20 times as long for the particles to become monodisperse (GSD < 1.1) as it does to reach d_{crit}, in reasonable agreement with prior calculations.[27] Critical

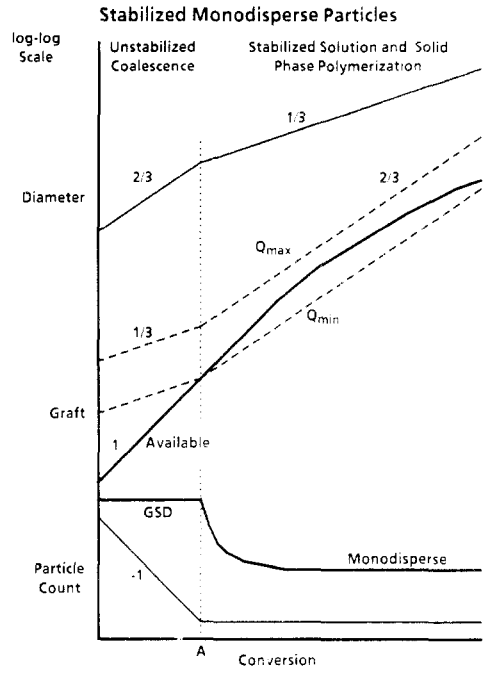

Figure 2. Schematic representation of the scaling of several important quantities during dispersion polymerizations generating monodisperse final particles. To the left of point A, the reaction is unstabilized; to the right, the particles are stabilized. The numbers appearing above the lines refer to the slope, or scaling.

sizes on the order of 10^5–10^8 polymer chains (around 0.1 μm) lead to particle counts consistent with final particle sizes in the 1–10-μm range.

What Determines d_{crit}? We submit that d_{crit} is determined by the grafting mechanism of stabilization. The critical point occurs when the graft available equals the minimum graft required to stabilize the particles. The amount of graft available increases linearly with conversion for as long as solution polymerization is dominant. On the other hand, the minimum amount of graft required to stabilize the particles depends on the total surface area of the particles times some minimum coverage by graft required to stabilize a unit of particle surface, Q_{min}.

We can now chart some of these fundamental relationships in Figure 2, which is a log–log plot of several quantities during dispersion polymerization. In the beginning of the reaction, when most polymerization takes place in solution, the situation to the left of point A is expected: the polymerization is unstabilized, particle diameter increases as the 2/3 power of conversion, particle count decreases, and the GSD is large, but constant. The total surface area of the particle ensemble grows with $N_p \times d^2$, so the dashed line representing the minimum graft required (labeled Q_{min}) increases with a slope of 1/3, while the amount of graft available increases with a slope of 1. Q_{max} describes the situation above which the particle surface is saturated and cannot accept more graft. When the amount of graft available equals the minimum graft required, then, by definition, the particles become stabilized (at point A).

Once stabilized, the particles may grow by polymerization both inside and outside the particle. Polymer that terminates in solution is unstable with respect to coalescence and is scooped up by the larger, stabilized particles before it can become stabilized as secondary particles. Because the grafting probability is low, secondary particles would have to be large before becoming stabilized and are usually captured by larger particles before they can become large enough. In the growth regime to the right of point A in Figure 2, the number of particles is fixed and the diameter now increases with the 1/3 power of conversion, so Q_{min} and Q_{max} coverage requirements increase with the 2/3 power of conversion. The aggregative mechanism of growth (capture of oligomeric free radicals or dead polymer from solution) results in a narrowing of the size distribution, and the GSD quickly declines. This narrowing of the size distribution can be simulated, as seen in Figure 1, or compared to interval II kinetics in the case of emulsion polymerization.[21]

As the reaction progresses well beyond the critical point A, the relative importance of solution polymerization may decrease as solid-phase polymerization becomes significant. When this occurs, the amount of graft being generated will also decrease, because it is only formed in solution (the stabilizer polymer is not soluble inside the particles). However, as long as the total graft available remains between the lower and upper coverage bands, Q_{min} and Q_{max}, the particle distribution can remain monodisperse.

Prediction of Particle Size. Given the multibin particle aggregation model for the unstabilized reaction and the relationships sketched in Figure 2, we can see that if we could predict Q_{min} and the amount of graft available, we could predict the particle size. The graft available equals the product of the number of chains formed thus far ($k_1 t$) times the probability of grafting. If grafting occurs by chain transfer to stabilizer, then the probability of grafting is given by $C_s[S](CL)/[M]$, as shown in eq 11.[29]

$$\text{graft available} = k_1 t \frac{C_s[S](CL)}{[M]} = C_s[S] N_A x \qquad (11)$$

The graft required is given by the total surface area times Q_{min}:

$$\text{graft required} = N_p \pi d_{50}^2 Q_{min} = \frac{6[M]MW_s Q_{min} x}{\rho d_{50}} \qquad (12)$$

The critical point occurs when the graft available equals the minimum graft required (eq 13, where $d_{crit} = d_{50}$)

$$d_{crit} = \frac{6[M]MW_s Q_{min}}{\rho C_s[S] N_A} \qquad (13)$$

The critical conversion, x_{crit}, can be obtained from eqs 13 and 8:

$$x_{crit} = d_{crit}^{3/2} \left(\frac{0.386 \pi \rho N_A k_p}{6[M]MW_s k_2} \right)^{1/2} \left(\frac{f k_d [I]}{k_t} \right)^{1/4} \qquad (14)$$

Providing the number of particles becomes fixed at the stabilization point, the final particle size, d_f, at the end of the reaction (*irrespective of the mechanism of growth subsequent to stabilization*) is given by eq 15, and by substitution, eq 16.

$$d_f^3 = d_{crit}^3 / x_{crit} \qquad (15)$$

$$d_f = \left(\frac{6[M]MW_s}{\rho N_A} \right)^{2/3} \left(\frac{Q_{min}}{C_s[S]} \right)^{1/2} \left(\frac{k_2}{0.386 \pi k_p} \right)^{1/6} \times \left(\frac{k_t}{f k_d [I]} \right)^{1/12} \qquad (16)$$

Equation 16 predicts the final particle size from first principles.

Methods of Estimation of Q_{min} and Q_{max}. To develop a priori predictions of particle size from dispersion polymerization where the grafting mechanism of steric sta-

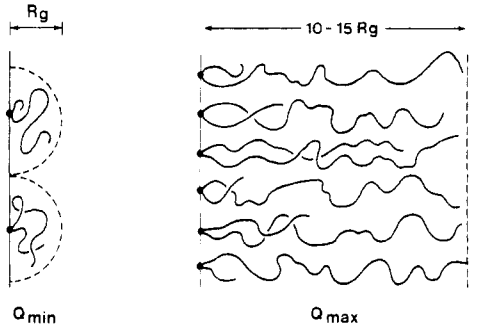

Figure 3. Qualitative picture of the graft coverage represented by Q_{min} and Q_{max} (de Gennes "mushroom" and "brush", respectively[30]).

bilization is operative, we require an estimate for Q_{min}, the minimum coverage by graft required to prevent coalescence. This quantity is likely related to the area of the shadow cast by the hemisphere defined by the radius of gyration of the stabilizer chains in solution, R_g (eq 17; Figure 3).[30] The radius of gyration of the grafted stabilizer chains will be smaller than that for an ungrafted stabilizer in solution because the point of attachment to the particle may occur anywhere along the chain. Thus, the longer end will dominate R_g, so the average chain length of the long stabilizing end will be 75% of the molecular weight of the ungrafted stabilizer. Therefore, the usual expression $R_g = AM_w^b$ for an ungrafted stabilizer becomes $R_g = A(0.75M_w)^b$, leading to the second half of eq 17.

$$Q_{min} = \frac{1}{\pi R_g^2} = \frac{1}{\pi A^2 (0.75M_w)^{2b}} \tag{17}$$

At the other extreme, adsorption of block copolymers onto mica surfaces has shown chain extensions up to $10–15R_g$ for flexible polymers in good solvents,[31,32] so one might infer Q_{max} is approximately $10–15Q_{min}$. Values closer to perhaps 10× are more likely because of the interference of the shorter end of the graft, which is held nearer the surface, on average, than the longer end.

Substituting eq 17 into eq 16 gives a model expression accounting for many of the factors influencing particle size.

$$d_f = \left(\frac{1}{0.75^b A M_w^b}\right)\left(\frac{6[M]MW_s}{\rho\pi N_A}\right)^{2/3}\left(\frac{1}{C_s[S]}\right)^{1/2} \times \left(\frac{k_2}{0.386k_p}\right)^{1/6}\left(\frac{k_t}{fk_d[I]}\right)^{1/12} \tag{18}$$

It is now possible to test the predictions inherent in eq 18 in two ways: (a) by comparing the predicted absolute value of particle size to experiment and (b) by comparing the predicted scaling of particle size to experiment.

Prediction of Absolute Particle Size. For the polymerization of 15% styrene with 1% AIBN in ethanol at 70 °C in the presence of 15 g L^{-1} of PVP (MW = 40 000),[6,16] the fixed constants take on the following values: [M] = 1.3 mol L^{-1}, MW_s = 104 g mol^{-1}, ρ = 1.0 g cm^{-3}, N_A = 6.0×10^{23} mol^{-1}, [I] = 8.2×10^{-3} mol L^{-1}, [S] = 0.135 mol of PVP units L^{-1}, and M_w = 40 000. The other known constants from the literature are $A = 5.3 \times 10^{-8}$ cm mol g^{-1} (ref 33; in methanol), b = 0.32 (ref 33; in methanol), $k_t = 6.1 \times 10^7$ L mol^{-1} s^{-1} (ref 1), k_p = 352 L mol^{-1} s^{-1} (ref 1), f = 1.0 (assumed; ref 29), and $k_d = 3.2 \times 10^{-7}$ s^{-1} (ref 34).

This leaves only C_s and k_2 requiring estimate. Chain transfer to PVP stabilizer can be approximated by the chain-transfer constant for dimethylformamide ($(1–4) \times 10^{-4}$) or 4-hydroxybutyric acid lactone (0.4×10^{-4}) as being ca. 10^{-4} (ref 35). With the kinetic parameters described above, the probability of polystyrene grafting to PVP is approximately one chain in 100. The rate constant k_2 employed in the multibin particle coalescence model refers to the rate of coalescence of single-chain hard spheres. On the basis of comparisons to small-molecule chemistry, diffusion-controlled processes have rate constants on the order of $10^8–10^{10}$ L mol^{-1} s^{-1}. We chose 10^9, but an error of an order of magnitude affects d_f by <50%, due to the low scaling power (1/6) in eq 18.

Substituting the above values into eqs 16–18 produces the following calculated values: $Q_{min} = 1.5 \times 10^{11}$ grafts cm^{-2} (1500 per μm^2; 110 per d_{crit} particle; R_g = 14 nm; coverage = 0.1 mg of PVP m^{-2}), d_{crit} = 0.15 μm, $x_{crit} = 8.8 \times 10^{-5}$ (0.009%; 44 s), and d_f = 3.4 μm.

Although only envisaged as an order of magnitude estimate, the final value for d_f is in remarkable agreement with experiment (3.0 μm; ref 6). The model is consistent with the framework of assumptions from which it was derived: the number of particles is determined within the first fraction of a percent conversion, where solution polymerization dominates and the volume fraction of polymer is too low to support significant solid-phase polymerization.

The calculated minimum graft coverage (0.1 mg of PVP m^{-2}) is in good agreement with reported maximum adsorption coverage of homopolymers and block copolymers (1–3 mg m^{-2}; refs 37–39), after adjustment for the expected factor of 10 difference between minimum and maximum coverage. A radius of gyration of 5–20 nm for the stabilizer chains is not likely to hinder approach and coalescence of 10-nm, graft-free secondary polystyrene particles of 1–20 chains, so growth by accretion of dead polymer formed in the continuous phase can continue, even though same size particle coalescence stops above d_{crit}. Of course, the critical point is unlikely to be the sharp discontinuity idealized in Figure 2 and may well be rounded off, particularly if coalescence probability is not diffusion controlled, but rather a continuous function of coverage. However, even in such a more realistic scenario, the approximate location of the critical point, and especially the critical size, can be determined by the intersection of lines of approach and departure—equivalent to the present analysis.

As noted before, it takes about 20 times as long for the stabilized particles to narrow their distribution as it takes to reach the critical size, so by 0.2% conversion, this model predicts, the particles in this example will be monodisperse. This is fully consistent with the first observed particles at 2–5% conversion, which are already monodisperse. Extremely rapid arrival at the critical conversion also highlights the sensitivity of the final particle size to the initial temperature. If the reaction mixture has not reached thermal equilbrium by the time of initiation, the rate of initiation could be much lower, and the particle size correspondingly smaller. This may account for large differences in particle size observed for the same recipe run in different laboratories[5] and may present a compelling argument for leaving the inhibitor in the styrene, so that the postponement of polymerization assists achievement of thermal equilibrium. Furthermore, this feature makes it extremely difficult to measure early particle growth kinetics prior to the critical point, although, perhaps, a flow system could be employed.

In absolute terms, the preceding model is remarkably consistent with experiment, providing reasonable predictions within a factor of 2 of measured quantities. How-

Table I
Predicted and Observed Scaling of Particle Size

parameter	predicted power law dependence: full adsorption model (eq 18)	predicted power law dependence: partial adsorption model (eq 20)	obsd power law dependence for PVP[a]
stabilizer concn [S]	−0.50	−0.50	−0.3
stabilizer mol wt	$-b$ (PVP: −0.32)[b]	$(1 - 2b)/2$ (PVP: 0.17)	−0.18
initiator concn [I]	−0.08	0.17	0.4
monomer concn [M]	0.67	$0.17/\exp(\Delta\delta^2/2)$	>1, but mostly a solvent effect

[a] Reference 6. [b] Reference 33.

ever, a more demanding test of the adequacy of the model would be a comparison of the predicted scaling of particle size with reaction parameters such as monomer, initiator, and stabilizer concentration and stabilizer molecular weight. However, it has been noted before that the major effect on dispersion-polymerized particle size is the effect of solvent,[4,6] which is only poorly accounted for by eq 18. Therefore, quantitative analysis of the scaling laws requires some prior consideration of the fraction of graft adsorbed onto the particles.

Fraction of Graft Adsorbed. For simplification, the preceding discussion had assumed that all graft formed was immediately adsorbed onto the particle surface. This may be the case in polar solvents such as methanol or ethanol (as in the foregoing numerical example) but is likely not the case in solvents generating larger particles (butanol,[6] ethanol/toluene mixtures,[4] ethanol/methoxyethanol mixtures,[15] etc.). Lower molecular weight polystyrene and grafted polystyrene are likely to have a finite solubility in these better solvents, especially in the presence of a significant volume fraction of monomer in the starting reaction mixture. For example, Ober and Lok found the polystyrene solubility limit to be between 9000 and 17 000 in 50/50 ethanol/methoxyethanol.[15] When grafted to stabilizer, solubilization of even longer chains might be possible.

To incorporate the role of solvent in dispersion polymerization in terms of changes in the solubility of graft, it is necessary to introduce the concept of F_a: the fraction of graft that is actually adsorbed onto the particles under conditions near the stabilization point. The main contributors to F_a are likely to be the molecular weight ratio of polymer to stabilizer (MW_p/M_w) and the effect of solvency, represented here by an ill-defined $\exp(\Delta\delta^2)$ term, where $\Delta\delta$ refers to the (presumably multidimensional) solubility parameter difference between the solvent and the graft.[4,40] Other contributors include the influence of molecular weight dispersity of both the polystyrene and steric stabilizer. For example, the hydrodynamic thickness of adsorbed polymers may depend on the high molecular weight tails of the distribution.[36]

As a first-order, intuitive approximation, intended to illustrate how F_a can greatly influence the scaling of the final size, we imagine the adsorption isotherm to be such that, where $F_a < 1$, F_a incrases linearly with both the molecular weight ratio and the solvent term, as suggested by eq 19. Thus, the thermodynamic probability of adsorption increases as the polystyrene molecular weight increases and as the difference in solubility parameters increases. Substituting for MW_p in terms of chain length (eq 8), we obtain the full expression in eq 19.

$$F_a = K\frac{MW_p}{M_w}e^{\Delta\delta^2} = \frac{Kk_p[M]MW_s}{M_w(k_t f k_d[I])^{1/2}}e^{\Delta\delta^2} \qquad (19)$$

This F_a is introduced into the theory as a multiplicative factor in eq 6 and emerges with an exponent of $-1/2$ in eq 16. More significantly, F_a brings with it additional dependency on monomer and initiator concentrations as well as on the molecular weight of stabilizer, generating eq 20.

$$d_f = \frac{1}{0.75^b A}\left(\frac{6}{\pi\rho N_A k_p}\right)^{2/3}\left(\frac{M_w^{1-2b}}{C_s[S]Ke^{\Delta\delta^2}}\right)^{1/2} \times \left(\frac{k_t^2 k_2 f k_d[I][M]MW_s}{0.386}\right)^{1/6} \qquad (20)$$

Although crude, eq 20 gives a second set of scaling laws we can compare to experiment.

3. Comparison of Predicted and Experimental Scaling

The preceding discussion has generated two models that predict particle size as a function of reaction parameters: eq 18 represents 100% graft adsorption, while eq 20 represents a highly simplified fractional graft adsorption model. Table I summarizes the predicted scaling of particle size for each, comparing them to the observed coefficients for the PVP-stabilized dispersion polymerization of styrene in polar solvents, as resported in the preceding paper.[6]

Effect of Stabilizer Concentration. The predicted exponent for the dependence of particle diameter on stabilizer concentration, [S], is −0.5 in both models, while values around −0.3 were reported in the preceding paper.[6] Values from 0.2 to 1.0 have been reported in the literature,[7,41] although some of these exponents refer to block copolymer or comb stabilized dispersion polymerizations, where the grafting mechanism of stabilization may not be operative and much smaller particles are obtained. Experimental results from our laboratory on HPC-stabilized dispersion polymerizations are consistent with an exponent of ca. −0.5 (although not all these particles were monodisperse).[1,18] In any event, the grafting model of stabilization predicts an exponent in much better agreement with experiment than the value of −1 expected for a homopolymer adsorption mechanism.

Effect of Stabilizer Molecular Weight. Table I shows the two models predict significantly different, but small scaling exponents for particle size dependence upon stabilizer molecular weight. The observed value for PVP-stabilized dispersion polymerization falls between the two predicted values, being somewhat closer to the simpler full adsorption model of eq 18. There is little comparable literature, except for Corner's work on PAA-stabilized dispersion polymerization of styrene in ethanol/water, where he found no effect of stabilizer molecular weight over the range 4000 to 10^6 Da,[12] and our work showing little effect of HPC molecular weight over the range 64 000–300 000, where somewhat larger particles were observed at an intermediate molecular weight.[18]

Effect of Initiator Concentration. With either model described above, the effect of initiator concentration on particle size is forecast to be extremely small and is much lower than the exponent of 0.4 observed by us[6] and by Vanderhoff and El-Aasser.[16] In order to get an expo-

nent of 0.4 from this model, we would have to hypothesize that F_a was proportional to the square of the molecular weight of the polystyrene block in the graft or that chain transfer to initiator was significant (which it may be[1]).

Effect of Monomer Concentration. The effect of monomer concentration predicted by the two models is quite different, although both models forecast a significant effect (Table I). The observed scaling coefficient may be slightly larger than 1.0 but has been noted to be primarily a solvent effect, so direct comparison with the partial adsorption model is difficult in the absence of good $\Delta\delta^2$ information.

Solvency Effects. In the context of this model, the primary effect of solvency is on the graft available line in Figure 2. As the dissolved graft content increases, the line for "graft available" in these figures will decrease, increasing the critical and final particle sizes.

Temperature Effects. The effect of temperature on the sizes of dispersion-polymerized particles has been little investigated in the literature, although it appears that larger particles are obtained at higher temperatures.[42] The effect of temperature is predicted to be felt through the various rate constants in eq 18 or 20, with d ln d_f/d $(1/T)$ giving an apparent activation energy $E_a' = (2E_{a2} - 2E_{ap} + E_{at} - E_{ad})/12$ for eq 18 (ignoring smaller influences on R_g and $\Delta\delta^2$). The activation energies for coalescence, polymerization, and termination are rather low, in comparison to E_{ad} for initiator decomposition. Thus increasing temperature increases the size by increasing k_d proportionately more than the other rate constants.

4. Limits to Particle Growth: Multimodal Particle Size Distributions

The preceding models describe the number of particles formed when the final product is monodisperse. The number of particles is fixed in the first 0–2% conversion, determined by the initial solvency, initiator concentration, and temperature as well as stabilizer concentration and molecular weight. Even when the solvency changes substantially during reaction, the monodisperse size distribution may be maintained as long as all freshly nucleated new material formed by solution polymerization is scavenged by existing particles and does not have an opportunity to accumulate with other new nuclei and become stabilized by grafted stabilizer.

As noted in the development of these models, secondary nucleation may occur when the surface graft coverage exceeds Q_{max} (which might be ca. 10 times Q_{min}). Such a range for graft coverage permits a growth of ca. a factor of 10 in diameter from the critical point, d_{crit}, by solution polymerization only. If solid-phase polymerization can occur as well, the generation of graft may be slowed relative to the generation of surface area, permitting even larger growth factors from d_{crit}. This is likely why the sample calculation of d_f can parallel observation: the 20× growth from d_{crit} to d_f (0.15–3.5 μm) is accompanied by a gel effect indicative of significant solid-phase polymerization.[1] In experiments designed to monitor particle growth or to grow larger particles from 1–5-μm seeds, one seldom observes retention of monodispersity for more than a factor of 10 in diameter.[18]

Two kinds of breakdown of monodispersity have been observed in dispersion polymerization: stabilization of secondary particle populations, and large particle coalescence.[1,4,6,18]

Secondary Stabilization. Figure 4 portrays the situation when the amount of graft available increases to the point where it exceeds the surface capacity, Q_{max}.

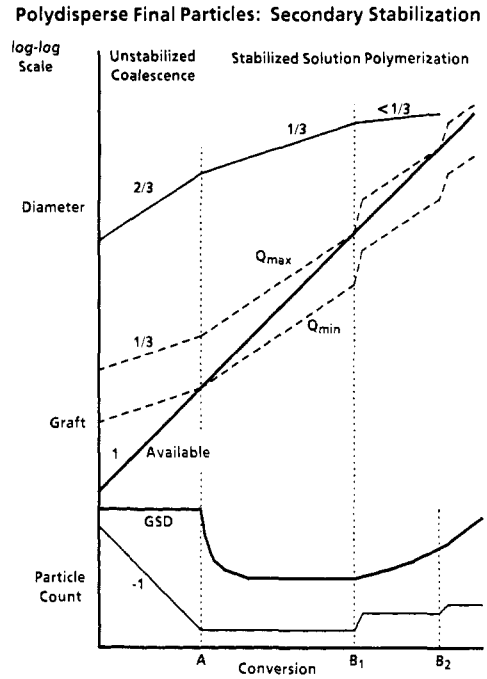

Figure 4. Schematic representation of the loss of monodispersity due to secondary and tertiary stabilization at points B_1 and B_2. Such an outcome is more likely when solution polymerization remains dominant throughout the reaction, so the graft available exceeds Q_{max}.

Excess graft cannot be accommodated on the existing particles and is expelled from them (or, possibly buried inside, if expulsion is not possible). If excess graft is expelled, it may be able to stabilize a second crop of smaller particles growing from dead chains formed in solution but not yet captured by the large particles. In this case, the stabilized particle number count will increase, the size distribution will broaden, and the original particles will grow more slowly, as shown in the figure. Immediately after secondary stabilization, new Q_{min} and Q_{max} requirements will be established for each population. The term most accurately describing this situation is "secondary stabilization" rather than "secondary nucleation". Nucleation appears to be continuous throughout the reaction, but once the particles become stabilized, they can capture subsequent nuclei before the new arrivals become stabilized themselves.

There are many examples of secondary stabilization in HPC-stabilized dispersion polymerization of styrene.[1,4,6,18] Some reactions produced particles with as many as four identifiable populations. The monodisperse component was often the largest, and the second and third populations had wider size distributions than the original monodisperse component—probably because they began life only partially stabilized and had to compete with the established particles for graft and monomer. Generally, secondary stabilization and wider size distributions prevail in the HPC-stabilized system[13–15,19,42] to a greater extent than in the PVP-stabilized system,[5,6,16,20] giving the impression of a narrower operating window for monodisperse particle synthesis with HPC. One possible reason for this could be that HPC is stiff and rodlike[43] and may prefer to lie somewhat tangentially on the particle surface, while PVP is more flexible and can extend further into solution. If HPC were tangentially oriented, then Q_{max}/Q_{min} may be lower than for PVP, so the amount of graft available may overshoot the upper bound more readily.

Large-Particle Coalescence. This second common type of polydisperse particle distribution may result if

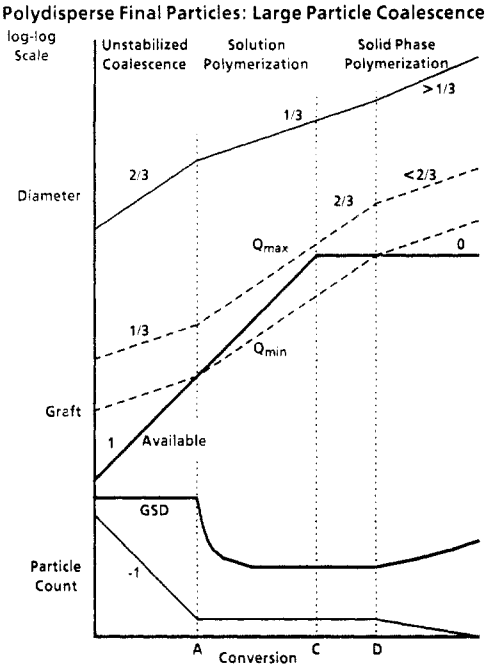

Figure 5. Schematic representation of the loss of monodispersity by large-particle coalescence at point D. This may occur if solid-phase polymerization becomes dominant at an intermediate point, C, and graft is no longer generated.

there is too complete a changeover from solution polymerization (the only source for graft) to inside polymerization. As Figure 5 indicates, such a changeover may result in the graft available line emerging below the minimum coverage requirement late in the reaction, resulting in some degree of coalescence. In this case, the particle count decreases, the average diameter increases a little faster, and the size distribution broadens.

5. Summary and Concluding Remarks

Figures 2, 4, and 5 sketch out a mechanistic model for dispersion polymerization where the ideal monodisperse particles are obtained in a window between extremes of large-particle coalescence and secondary stabilization. The key controlling parameters in this model are the availability of graft and the minimum and maximum coverage, Q_{min} and Q_{max}. The balance between solid-phase and solution-phase polymerization subsequent to stabilization must be steered carefully to prevent either secondary particle formation or large-particle coalescence.

Equations 18 and 20 were derived to predict the monodisperse final particle size from first principles, in the case of full adsorption of graft and a specific simple model for partial adsorption of graft, respectively. Comparison with experiment indicates that partial adsorption of graft is most likely and that the simple model of eq 19 does not fully account for it, leaving some residual discrepancies between observed and predicted scaling of particle size with reaction parameters.

This model is valid when grafting is the mechanism of steric stabilization and when graft can rearrange to situate on the particle surface at all times. It provides a reasonable description of HPC-, PVP-, PAA-, and likely poly(vinylbutyral)- and poly(*N*-vinylpyridine)-stabilized polymerizations of styrene in polar solvents.[1-6,12-20,42] The model is also expected to apply when polymerizable "macromonomers" are employed as prestabilizers, and end up grafted to the particle surface.[44] However, detailed experimental data relating to the influence of reaction parameters on macromonomer-stabilized particle size has not been reported.

The model may also apply to poly(isobutylene)-stabilized polymerization of methyl methacrylate or poly(2-ethylhexyl acrylate)-stabilized polymerization of vinyl acetate in hydrocarbons, where Winnik et al. have shown the particle structure to comprise a networked interphase of stabilizer throughout the particle.[10,11,45-50] However, in order to apply to these latter reactions, the early particles would need to be surface stabilized, and the particle count would have to be determined before crosslinking anchored the graft, leaving microstructure formation as the only option for growing particles above Q_{max}. An interesting case intermediate to the extremes of the Winnik systems and our system is polymerization of methyl methacrylate in alcohols, currently under investigation by Vanderhoff and El-Aasser.

The present model does not apply to other types of dispersion polymerization where pregrafted comb or block copolymer stabilizers are active.[7,8,41] In these cases, the particles are often much smaller because much more of the true stabilizer is available. In some reactions employing such stabilizers, however, the particle size dependence on stabilizer concentration is often not consistent with simple adsorption, suggesting that grafting may also occur. Additionally, surface curvature in cases where R_g becomes comparable to d_{crit} may be a factor influencing the scaling in the case of very small particles.

At its present level of development, this model presents the framework for a complete description of the system. The coalescent concepts could be more realistically defined, perhaps in terms of a coverage-dependent coalescence probability, analogous to the Fuchs stability ratio for electrostatically stabilized particles.[47] Such refinements, however, would only serve to round out the sharp break at point A in Figures 2, 4, and 5, although incoming and exiting slopes, and therefore, the ultimate particle size predictions and scaling, should remain the same.

The present model has not directly addressed the prediction of molecular weight. However, given the prediction of particle size as a function of conversion, this model, considerations cited in our previous paper,[6] and the thermodynamic model of Vanderhoff and El-Aasser for the distribution of monomer, initiator, and solvent inside and outside the particles[20] could be combined with appropriate polymerization kinetics models for each phase to forecast the extent of solution and solid-phase polymerization, and hence the expected molecular weight.

Glossary Notation

A	proportionality constant for the relation $R_g = AM_w^b$
b	exponent relating radius of gyration to molecular weight
C_s	chain-transfer constant for transfer to stabilizer (per monomer unit)
CL	chain length (in monomer units)
d	particle diameter
d_{50}	volume median diameter
d_{crit}	critical diameter, above which same size particle coalescence is no longer possible
d_f	final particle size
$\Delta\delta^2$	difference in multidimensional solubility parameters between the solvent and grafted stabilizer
D	diffusion constant
E_a'	apparent activation energy, the slope of d ln d_f/d(1/T)
E_{a2}	activation energy for particle coalescence, k_2
E_{ad}	activation energy for initiator decomposition, k_d

E_{ap} activation energy for polymerization of styrene, k_p
E_{at} activation energy for termination of styrene polymerization in solution, k_t
f fraction of initiator fragments forming radicals
F_a fraction of graft that is adsorbed onto the particle surface
GSD geometric standard deviation of the size distribution
i bin index
[I] initiator concentration (in mol L^{-1})
j bin index
k_1 pseudo-zero-order rate of dead chain generation (in mol L^{-1} s^{-1})
k_2 diffusion-controlled rate constant for coalescence of similar-sized particles (in L mol^{-1} s^{-1})
k_d rate constant for initiator decomposition (in s^{-1})
k_{ij} second-order rate constant for coalescence of particles in bin i with particles in bin j
k_p polymerization rate constant (in L mol^{-1} s^{-1})
k_t termination rate constant (in L mol^{-1} s^{-1})
K proportionality constant for dependence of F_a on molecular weight ratio and solvency term (eq 19)
m_j total mass of particles in bin j (in units of polymer chains of length CL)
$\langle m_j^2 \rangle$ sum of the squares of the masses of particles in bin j
M overall weight-average particle mass (in units of polymer chains of length CL)
[M] monomer concentration (in mol L^{-1})
M_w molecular weight of stabilizer
MW_p molecular weight of polystyrene
MW_s molar weight of styrene (in g mol^{-1})
n_j number of particles in bin j
N overall number-average particle mass (in units of polymer chains of length CL)
N_A Avogadro's number
N_p number of particles per liter
R_g radius of gyration of stabilizer chains in solution
[S] concentration of stabilizer (in mol monomer units L^{-1})
Q_{min} minimum graft coverage required to stabilize particles against same-size coalescence (in grafts cm^{-2})
Q_{max} maximum graft coverage on saturated particles (in grafts cm^{-2})
ρ density (in g cm^{-3})
t time (in s)
T temperature (K)
x conversion
x_{crit} conversion at the critical point

References and Notes

(1) Paine, A. J. *J. Colloid Interface Sci.*, accepted.
(2) Paine, A. J.; Deslandes, Y.; Gerroir, P.; Henrissat, B. *J. Colloid Interface Sci.*, accepted.
(3) Winnik, F. M.; Paine, A. J. *Langmuir* **1989**, *5*, 903.
(4) Paine, A. J. *J. Polym. Sci., Part A: Polym. Chem.*, accepted.
(5) Paine, A. J.; McNulty, J. *J. Polym. Sci., Part A: Polym. Chem.*, accepted.
(6) Paine, A. J.; Luymes, W.; McNulty, J. *Macromolecules*, accompanying paper in this issue.
(7) Barrett, K. E. J., Ed. *Dispersion Polymerization in Organic Media*; Wiley-Interscience: New York, 1975.
(8) (a) Dawkins, J. V.; Shakir, S. A.; Croucher, T. G. *Eur. Polym. J.* **1987**, *23*, 173. (b) Dawkins, J. V.; Maghami, G. G.; Shakir, S. A.; Higgins, J. S. *Polym. Prepr. (Am. Chem. Soc., Div. Polym. Chem.)* **1985**, *26*, 234. (c) Dawkins, J. V.; Taylor, G.; Baker, S. P.; Collett, R. W. R.; Higgins, J. S. *ACS Symp. Ser.* **1981**, *No. 165*, 189.
(9) (a) Croucher, M. D.; Winnik, M. A. *NATO ASI Ser. C*, in press. (b) Winnik, M. A.; Lukas, R.; Chen, W. F.; Furlong, P.; Croucher, M. S. *Makromol. Chem., Macromol. Symp.* **1987**, *10/11*, 483.
(10) Williamson, B.; Lukas, R.; Winnik, M. A.; Croucher, M. D. *J. Colloid Interface Sci.* **1987**, *119*, 559.
(11) Egan, L. S.; Winnik, M. A.; Croucher, M. D. *Polym. Eng. Sci.* **1986**, *26*, 15.
(12) Corner, T. *Colloids Surf.* **1981**, *3*, 119.
(13) Ober, C. K.; Lok, K. P. *Macromolecules* **1987**, *20*, 268.
(14) Ober, C. K.; Lok, K. P.; Hari, M. L. *J. Polym. Sci., Polym. Lett. Ed.*, **1985**, *23*, 103.
(15) Lok, K. P.; Ober, C. K. *Can. J. Chem.* **1985**, *63*, 209.
(16) Tseng, C. M.; Lu, Y. Y.; El-Aasser, M. S.; Vanderhoff, J. W. *J. Polym. Sci., Part A: Polym. Chem.* **1986**, *24*, 2995.
(17) Almog, Y.; Reich, S.; Levy, M. *Br. Polym. J* **1982**, *14*, 131.
(18) Paine, A. J. Presentation at Lehigh University, Oct 5, 1987.
(19) Ober, C. K.; van Grunsven, F.; McGrath, M.; Hair, M. L. *Colloids Surf.* **1986**, *21*, 347.
(20) Lu, Y. Y.; El-Aasser, M. S.; Vanderhoff, J. W. *J. Polym. Sci., Part B: Polym. Phys.* **1988**, *26*, 1187.
(21) (a) Piirma, I., Ed. *Emulsion Polymerization*; Academic Press: New York, 1982. (b) Vanderhoff, J. W. *J. Polym. Sci., Polym. Symp* **1985**, *No. 72*, 161.
(22) Hansen, F. K.; Ugelstad, J. *J. Polym. Sci., Part A: Polym. Chem.* **1978**, *16*, 1953.
(23) (a) Napper, D. H.; Gilvert, R. G. *Makromol. Chem., Macromol. Symp.* **1987**, *10/11*, 503. (b) Feeney, P. J.; Napper, D. H.; Gilbert, R. G. *Macromolecules* **1987**, *20*, 2922.
(24) Suzuki, A.; Ho, N. F.; Higuchi, W. I. *J. Colloid Interface Sci.* **1969**, *29*, 552.
(25) Marqusee, J. A.; Ross, J. *J. Chem. Phys.* **1984**, *80*, 536.
(26) Smoluchowski, M. V. *Z. Phys. Chem.* **1917**, *192*, 29.
(27) Frenklach, M. *J. Colloid Interface Sci.* **1985**, *108*, 237.
(28) Hildebrand, F. B. *Introduction to Numerical Analysis*; McGraw-Hill: New York, 1956.
(29) Flory, P. J. *Principles of Polymer Chemistry*; Cornell University Press: Ithaca, NY, 1953.
(30) (a) de Gennes, P.-G. *Adv. Colloid Interface Sci.* **1987**, *278* 189. (b) de Gennes, P.-G. *Macromolecules* **1980**, *138* 1069.
(31) Costello, B. A. de L.; Luckham, P. F.; Tadros, Th. F. *Colloids Surf.* **1988/1989**, *34*, 30.
(32) Marra, J.; Hair, M. L. *Colloids Surf.* **1988/1989**, *34*, 215.
(33) Ali, S.; Ahmad, N. *Br. Polym.* **1982**, *14*, 113.
(34) Brandrup, J.; Immergut, E. H., Eds. *Polymer Handbook*, 2nd ed.; Wiley-Interscience: New York, 1975.
(35) Bamford, C. H.; Tipper, C. F. H. *Free Radical Polymerisation* (Vol. 14A of *Comprehensive Chemical Kinetics*); Elsevier: New York, 1976.
(36) Cosgrove, T.; Vincent, B.; Crowley, T. L.; Cohen-Stuart, M. A. *ACS Symp. Ser.* **1984**, *No. 240*, 147.
(37) Ahmed, M. S.; El-Aasser, M. S.; Vanderhoff, J. W. *ACS Symp. Ser.* **1984**, *No. 240*, 77.
(38) Furusawa, K.; Kimura, Y. *ACS Symp. Ser.* **1984**, *No. 240*, 131.
(39) Cohen-Stuart, M. A.; Scheutjens, J. M. H. M.; Fleer, G. J. *ACS Symp. Ser.* **1984**, *No. 240*, 53.
(40) Barton, A. F. M., Ed. *Handbook of Solubility Parameters and Other Cohesion Parameters*; CRC Press: Boca Raton, FL, 1983.
(41) Susoliak, O.; Barton, J. *Chem. Pap.* **1985**, *39*, 379.
(42) Ober, C. K.; Hair, M. L. *J. Polym. Sci., Part A: Polym. Chem.* **1987**, *25*, 1395.
(43) Wirick, M. G.; Waldman, M. H. *J. Appl. Polym. Sci.* **1970**, *14*, 579.
(44) Ito, K.; Yokoyama, S.; Arakawa, F. *Polym. Bull.* **1986**, *16*, 345.
(45) (a) Winnik, M. A.; Williamson, B.; Russell, T. P. *Macromolecules* **1987**, *20*, 899. (b) Winnik, M. A. *Pure Appl. Chem.* **1984**, *56*, 1281. (c) Winnik, M. A.; Hua, M. H.; Hougham, B.; Williamson, B.; Croucher, M. D. *Macromolecules* **1984**, *17*, 262.
(46) (a) Peckan, O.; Winnik, M. A.; Egan, L.; Croucher, M. D. *Macromolecules* **1983**, *16*, 699. (b) Peckan, O.; Winink, M. A.; Croucher, M. D. *J. Polym. Sci., Polym. Lett. Ed.* **1983**, *21*, 1011.
(47) Fuchs, N. *Z. Phys.* **1934**, *89*, 736.

Registry No. Polystyrene, 9003-53-6.